FULL PAPER

A Bipolar Host Material Containing Triphenylamine and Diphenylphosphoryl-Substituted Fluorene Units for Highly Efficient Blue Electrophosphorescence

By *Fang-Ming Hsu, Chen-Han Chien, Ching-Fong Shu,* Chin-Hung Lai, Cheng-Chih Hsieh, Kang-Wei Wang,* and *Pi-Tai Chou**

Highly efficient blue electrophosphorescent organic light-emitting diodes incorporating a bipolar host, 2,7-bis(diphenylphosphoryl)-9-[4-(*N*,*N*-diphenylamino)phenyl]-9-phenylfluorene (POAPF), doped with a conventional blue triplet emitter, iridium(III) bis[(4,6-difluorophenyl)pyridinato-*N*,$C^{2'}$]picolinate (FIrpic) are fabricated. The molecular architecture of POAPF features an electron-donating (p-type) triphenylamine group and an electron-accepting (n-type) 2,7-bis(diphenylphosphoryl)fluorene segment linked through the sp^3-hybridized C9 position of the fluorene unit. The lack of conjugation between these p- and n-type groups endows POAPF with a triplet energy gap (E_T) of 2.75 eV, which is sufficiently high to confine the triplet excitons on the blue-emitting guest. In addition, the built-in bipolar functionality facilitates both electron and hole injection. As a result, a POAPF-based device doped with 7 wt% FIrpic exhibits a very low turn-on voltage (2.5 V) and high electroluminescence efficiencies (20.6% and 36.7 lm W^{-1}). Even at the practical brightnesses of 100 and 1000 cd m^{-2}, the efficiencies remain high (20.2%/33.8 lm W^{-1} and 18.8%/24.3 lm W^{-1}, respectively), making POAPF a promising material for use in low-power-consumption devices for next-generation flat-panel displays and light sources.

1. Introduction

Since the first report of organic light-emitting devices (OLEDs),[1] many studies have focused on improving their efficiency. Recently, phosphorescent OLEDs have attracted much attention because of their highly efficient performance relative to that of conventional singlet fluorescent OLEDs as a result of their harvesting of both singlet and triplet excitons for emission.[2–7] Phosphorescent emitters typically possess longer lifetimes for further diffusion, leading to undesired concentration quenching or T_1–T_1 annihilation and, thereby, declining performance.[8,9] To overcome this drawback, the triplet phosphor is usually doped into an appropriate host. Consequently, in the quest for efficient phosphorescent OLEDs, the development of effective host materials is as important as the development of the phosphors. There are some intrinsic physical requirements for the host materials: i) a triplet energy gap (E_T) larger than that of the triplet emitter, thereby preventing reverse energy transfer from the guest to the host;[10–15] ii) good carrier transporting properties that balance the charge fluxes and thus increase the opportunity for electron and hole recombination;[16–18] iii) highest occupied/lowest unoccupied molecular orbital (HOMO/LUMO) energy levels matching those of the adjacent layers, thereby reducing the operation voltage; iv) decent thermal and morphological stabilities, which extend the device's operational lifetime.[19,20] It is difficult, however, for a blue-light phosphorescent host to meet the requirements of a high-value E_T by confining the degree of π-electron conjugation in the host molecules while simultaneously conserving its charge transport properties. A restriction in the length of π-conjugation may result in a reduction of the carrier-injection/transport properties. To overcome this obstacle, a general design strategy is to incorporate a rigid charge-transporting group into the molecular structure of the host, for example, a carbazole unit for p-type hosts[21–25] and an aromatic phosphine oxide for n-type matrixes.[26–28] Nevertheless, the internal quantum efficiencies of devices using such p- or n-type hosts are significantly less than 100%—partly because of the injection and transport of a single carrier such that charge balance cannot be achieved in the emitting layer (EML).

Recent research trends have, therefore, turned to the development of hosts possessing bipolar properties.[28–33] Through the linking of both p- and n-type groups into the host's molecular structure, the carrier-injection/transport properties in the EML can achieve balanced charge fluxes, resulting in high device performance. In this study we synthesized a bipolar host,

[*] Prof. C.-F. Shu, F.-M. Hsu, C.-H. Chien
Department of Applied Chemistry
National Chiao Tung University
Hsinchu, 300 (Taiwan)
E-mail: shu@cc.nctu.edu.tw
Prof. P.-T. Chou, Dr. C.-H. Lai, C.-C. Hsieh, K.-W. Wang
Department of Chemistry
National Taiwan University
Taipei, 106 (Taiwan)
E-mail: chop@ntu.edu.tw

DOI: 10.1002/adfm.200900703

2,7-bis(diphenylphosphoryl)-9-[4-(*N*,*N*-diphenylamino)phenyl]-9-phenylfluorene (POAPF), that incorporates a p-type triphenylamine group linked to an n-type 2,7-bis(diphenylphosphoryl)-fluorene segment through the sp^3-hybridized C9 atom of the fluorene unit to effectively interrupt the conjugation of π-electrons. Instead of using a conventional p-type carbazole group, we chose triphenylamine as the building block for this blue phosphorescent host because the latter has a higher HOMO energy level than the former.[34] As a result, we expected POAPF-based devices to have reduced energy barriers for hole injection and thus lower operating voltages. Indeed, POAPF possesses four important characteristics: i) a high value of E_T because of the complete isolation of the π-electrons of the triphenylamine (E_T = ca. 3.04 eV)[35] and 2,7-bis(diphenylphosphoryl)fluorene units (E_T = ca. 2.72 eV, estimated from the methyl-substituted analogue)[27] provided by the nonconjugated linkage; ii) bipolarity, resulting from the coexistence of p- and n-type groups; iii) appropriate HOMO/LUMO energy levels, originating from the presence of electron-donating and accepting building blocks within the molecule; and iv) the capability of forming a stable amorphous thin film as a result of the molecule's bulky, nonplanar structure. Thus, we expected POAPF to act as a suitable host for blue phosphorescent emitters such as iridium(III) bis[(4,6-difluorophenyl)pyridinato-N,C^2]picolinate (FIrpic). To verify the bipolar properties of POAPF, we also prepared the corresponding p- and n-type-only compounds 9-[4-(*N*,*N*-diphenylamino)phenyl]-9-phenylfluorene (APF) and 2,7-bis(diphenylphosphoryl)-9,9-diphenylfluorene (PODPF), respectively.

2. Results and Discussion

2.1. Synthesis and Characterization

Scheme 1 illustrates the synthetic route that we followed to prepare the bipolar host compound POAPF. The starting material 2,7-dibromo-9-phenyl-9-fluorenol (**1**) was obtained according to procedures described in the literature.[36] An acid-promoted Friedel–Crafts-type substitution of **1** with triphenylamine yielded the key intermediate 2,7-dibromo-9-[4-(*N*,*N*-diphenylamino)-phenyl]-9-phenylfluorene (**2**). Lithiation of **2** with excess *n*-butyllithium and subsequent treatment with chlorodiphenylphosphine gave the phosphine-containing intermediate, which we converted to the target compound POAPF through oxidation with 30% aqueous hydrogen peroxide. To examine the influence of the built-in bipolar functionalities, we also synthesized the corresponding donor-only analogue APF and acceptor-only analogue PODPF. The final products were purified through column chromatography and sublimed prior to device fabrication. The molecular structures were characterized using ^1H, ^{13}C, and ^{31}P NMR spectroscopy, high-resolution mass spectrometry, and elemental analysis.

2.2. Thermal Properties

The thermal properties of POAPF, APF, and PODPF were characterized using thermogravimetric analysis (TGA) and differential scanning calorimetry (DSC). In the TGA measurements, POAPF and PODPF, which feature thermally stable diphenylphosphoryl groups,[37] exhibited high decomposition temperatures (T_d, corresponding to 5% weight loss) of 466 and 428 °C, respectively. These values are much higher than that (313 °C) of the phosphine oxide-free counterpart APF. The high temperature resistance of POAPF implied that it would be capable of enduring vacuum thermal sublimation, thereby meeting one basic requirement of a host to be used in OLEDs. The DSC traces of POAPF, APF, and PODPF exhibited distinct glass transition temperatures (T_g) during the second heating scans (scanning rate: 10 °C min^{-1}) (Fig. 1). We found that POAPF, with its one triphenylamine and two diphenylphosphine oxide groups at the 9- and 2,7-positions of the fluorene unit, respectively, exhibited the highest value of T_g among the three host materials. Such a molecular design not only renders a nonplanar molecular structure to hinder intermolecular interactions (i.e., close packing) but also increases the molecular rigidity, leading to a high value of T_g of 129 °C. We suspected that the high values of both T_d and T_g would make POAPF a thermally robust material that could bear the inevitable joule heating that occurs under device operation conditions.

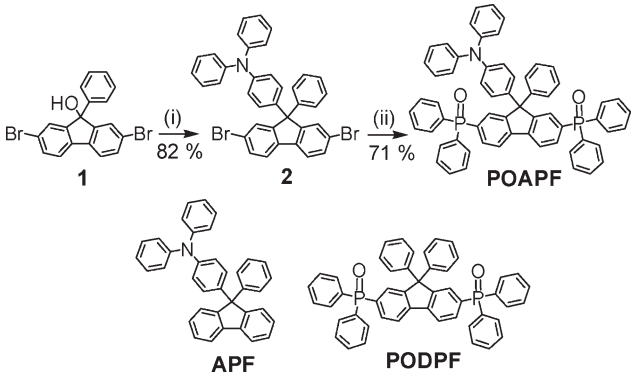

Scheme 1. Synthetic route toward POAPF and chemical structures of APF and PODPF. Reagents: i) triphenylamine, CF_3SO_3H, CH_2Cl_2; ii) a) *n*-BuLi, THF, b) PPh_2Cl, c) 30% $H_2O_{2(aq)}$, CH_2Cl_2.

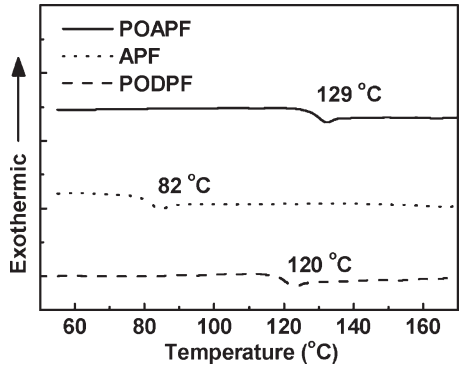

Figure 1. DSC traces of POAPF, APF, and PODPF recorded at a heating rate of 10 °C min^{-1}.

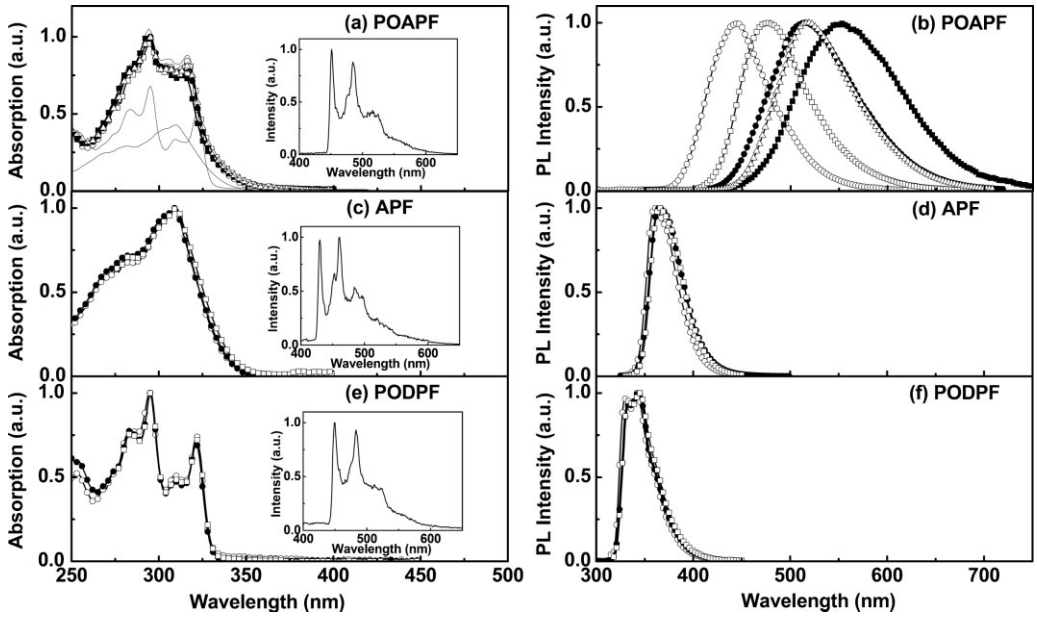

Figure 2. Room-temperature absorption and PL spectra of POAPF, APF, and PODPF (excited at 335, 310, and 320 nm, respectively) in cyclohexane (open circles), benzene (open squares), THF (closed circles), dichloromethane (open triangles), and acetonitrile (closed squares). Inset: phosphorescence spectra of POAPF, APF, and PODPF in frozen 2-methyltetrahydrofuran matrixes at 77 K (excited at 335, 310, and 320 nm, respectively). The solid lines in Figure 2a represent the respective absorption spectra of APF and PODPF in cyclohexane.

2.3. Photophysical Properties

Figure 2 depicts the UV–vis absorption and photoluminescence (PL) spectra of POAPF, APF, and PODPF in various organic solvents. Table 1 lists the pertinent photophysical and dynamic parameters. The steady-state absorption spectra of POAPF in, for example, cyclohexane (Fig. 2a) can be simulated qualitatively through a linear combination of the absorption spectra of APF and PODPF (Fig. 2a, solid line), with slight differences arising from summing the influences of two fluorene units (i.e., one each for APF and PODPF). As a result, we infer that only weak electronic coupling exists between the triphenylamine and 2,7-bis(diphenylphosphoryl)fluorene chromophores in POAPF in the ground state. In addition, we found that the features in the absorption spectra of POAPF are nearly independent of the solvent polarity. These results lead us to conclude that the Franck–Condon excited state is subject to a rather small dipolar change with respect to the ground state. In sharp contrast, the fluorescence maxima of the bipolar POAPF (Fig. 2b) revealed a remarkable bathochromic shift: from 442 nm in cyclohexane to 554 nm in acetonitrile. Furthermore, the excitation spectra (see Supporting Information, Fig. S1) were, within experimental error, effectively identical to the absorption spectra, indicating that the entire emission resulted from a common Franck–Condon excited state. For comparison, the unipolar compounds APF and PODPF, which contain solely a triphenylamine electron donor and a diphenylphosphoryl-substituted fluorene electron acceptor, respectively, exhibited normal Stokes-shifted emissions (366 nm for APF; 345 nm for PODPF; in tetrahydrofuran (THF)). In addition, their emission peaks underwent negligible shifts upon varying the solvent polarity (Fig. 2d and f).

Table 1. Photophysical properties of the hosts in various solvents.

host	solvent	λ_{abs} [nm]	λ_{em} [nm]	τ_{obs} [ns]	Φ
POAPF	cyclohexane	293. 305, 315	442	8.3	0.12
	benzene	394, 306, 316	473	23.5	0.10
	THF	294, 304, 315	515	24.0	0.07
	dichloromethane	294, 305, 315	517	42.5	0.06
	acetonitrile	293, 303, 314	554	16.7	0.01
APF	THF	309	366	2.1	0.13
PODPF	THF	295, 309, 321	345	1.9	0.98

To gain more insight into the emission spectral shift for POAPF, we prepared POAPF solutions in various solvents over the concentration range from 10^{-4} to 10^{-6} M. The resulting absorption spectra and emission profiles all exhibited concentration-independence, eliminating the possibility of the emission being caused by the formation of aggregates and/or excimers. Alternatively, given the p/n-type functionality in POAPF, the distinct solvatochromism may more plausibly be rationalized by a mechanism involving rapid photoinduced electron transfer (PET) within the bipolar POAPF molecule. The net result of such a PET process would be a large change in dipole moment in the excited state. In this case, the surrounding solvent molecules would exist in energetically unfavorable, non-equilibrium states that would then undergo dipole relaxation to the equilibrium polarization, resulting in solvent polarity-dependent emission, that is, fluorescence solvatochromism.[38,39] This hypothesis is supported by the strongly solvent-dependent shift in the signal in the emission spectrum depicted in Figure 2b. As a result, the change in magnitude of the dipole moment between the ground and excited states, that is, $\Delta\mu = |\vec{\mu}_e - \vec{\mu}_g|$, can be estimated using

the Lippert–Mataga equation

$$\tilde{\upsilon}_f = \tilde{\upsilon}_f^{vac} - \frac{2}{hc}(\vec{\mu}_e - \vec{\mu}_g)^2 a_0^{-3}\Delta f \quad (1)$$

where $\tilde{\upsilon}_f$ and $\tilde{\upsilon}_f^{vac}$ are the spectral positions (in wavenumbers) of the solvation-equilibrated emission maximum and the value extrapolated to the diluted gas phase, respectively, a_0 is the cavity radius in which the solute resides, estimated to be 7.4 Å at the B3LYP/6-31G* theoretical level,[40,41] h and c are Planck's constant and the speed of light, respectively, and Δf is the orientation polarizability, defined as

$$\Delta f = f(\varepsilon) - f(n^2) = \frac{\varepsilon - 1}{2\varepsilon + 1} - \frac{n^2 - 1}{2n^2 + 1} \quad (2)$$

where ε is the static dielectric constant and n is the optical refractivity index of the solvent. In Figure 3, the plot of $\tilde{\upsilon}_f$ as a function of Δf for POAPF is sufficiently linear, with a slope reaching as steep as $-12\,300\,cm^{-1}$. Accordingly, we calculated $\Delta\mu = |\vec{\mu}_e - \vec{\mu}_g|$ to be 22 D for POAPF, consistent with our hypothesis of charge transfer emission.

A further investigation of the dynamics of relaxation in various solutions firmly supported our proposed PET mechanism. In this study, we determined the fluorescence rise and decay dynamics of POAPF by using a time-correlated photon counting technique that provided a temporal resolution of ca. 15 ps. Figure S2 in the Supporting Information reveals that the decay traces were drastically different when monitoring the blue side and the red tail of the emission of POAPF in THF. Table 1 lists details of the associated photophysical parameters. Upon excitation at 350 nm, the decay (monitored at 400 nm) could be fitted well using two single-exponential components (<15 ps and 24 ns). Conversely, when we monitored on the red side of the signal (515 nm), only a single-exponential decay of 24 ns was evident—the rise component was beyond the response of the instrument of 15 ps. The fast decay of the <15-ps component at 400 nm, within experimental error, is consistent with the irresolvable rise time constant monitored at 515 nm, establishing a precursor/successor type of PET process. The identical population decay of the 24-ns component between the two wavelengths leads us to conclude the possible existence of overlap of the locally excited (LE) and charge transfer (CT) emission of POAPF at 515 nm in THF. In other words, at 400 nm we ascribe the decay component of <15 ps to the locally (Franck–Condon) excited emission, whereas we consider the 24-ns decay component originates from the charge transfer emission. In sum, the fast (<<15 ps) relaxation dynamics of the locally excited POAPF indicates the occurrence of a rapid PET process. This behavior is understandable because of the near proximity of the p-type (triphenylamine) and n-type (2,7-bis(diphenylphosphoryl)fluorine) chromophores in POAPF. Due to these charge transfer properties, we expected the associated emission to have a long population lifetime. This hypothesis is supported by the rather long emission lifetimes (several tens of nanoseconds; Table 1) in various solvents, with corresponding relatively small quantum yields (Φ; Table 1). The radiative lifetime τ_f can be deduced from the relationship

$$\tau_f = \tau_{obs}/\Phi \quad (3)$$

where τ_{obs} denotes the observed lifetime. According to the data listed in Table 1, we calculated that τ_f existed in a range from 70 ns to 1.6 μs, depending on the solvent polarity. In sharp contrast, the observed fluorescence lifetimes for the unipolar APF and PODPF in THF were as short as 2.1 and 1.9 ns, respectively, due to their originating from the locally excited donor (APF) and acceptor (PODPF) emissions. Assuming the PET efficiency of POAPF to be approximately unity, the solvent polarity-dependent yields ranging from 0.12 to 0.01 for POAPF are relatively small when compared with those of the parent molecules APF and PODPF. This phenomenon can be rationalized by considering that back-electron transfer is normally dominated by the radiationless deactivation. In addition, because the gap between the LE and CT energy levels increases upon increasing the solvent polarity, the radiative decay rate of the electron transfer band decreases as a result of the reduction in LE/CT electronic coupling.[42] The combination of these two factors can, therefore, be used to rationalize the decrease in the charge transfer emission quantum yield upon increasing the solvent polarity.

Figure 4 presents the PL spectra (excited at 335 nm) of POAPF films doped with various concentrations of FIrpic. The 7 wt%

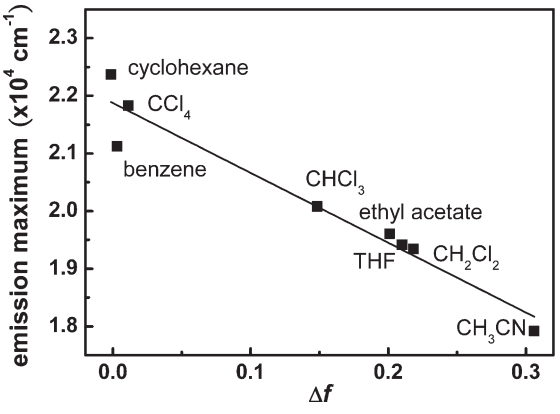

Figure 3. Lippert plot of the emission maximum ($\tilde{\upsilon}_f$) with respect to the orientation polarizability (Δf) of POAPF in various solvents.

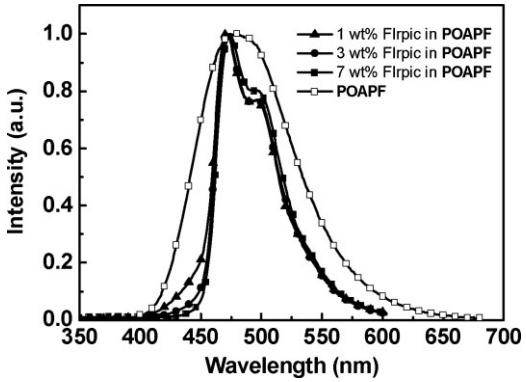

Figure 4. PL spectra (excited at 335 nm) of POAPF films doped with various concentrations of FIrpic (30 nm, formed on quartz substrates through thermal evaporation).

FIrpic-doped film exhibited only the blue emission from the dopant, suggesting complete energy transfer of singlet excitons from POAPF to FIrpic. The insets to Figure 2 depict the phosphorescence spectra of POAPF, APF, and PODPF in 2-methyltetrahydrofuran at 77 K. From the highest-energy 0-0 phosphorescence emissions, we estimate that their values of E_T are 2.75, 2.88, and 2.76 eV, respectively. We attribute the maintained high value of E_T of POAPF to the effective lack of conjugation between the triphenylamine and bis(diphenylphosphoryl)fluorene groups. Because POAPF possesses a higher value of E_T than that of FIrpic (2.62 eV), we would expect that i) the energy of the triplet excitons would be transferred effectively from the host to the guest emitter and ii) the reversing pathway was prohibited.

2.4. Electrochemical Properties

We investigated the electrochemical characteristics of POAPF, APF, and PODPF in solution through cyclic voltammetry (CV) using tetrabutylammonium hexafluorophosphate ($TBAPF_6$) as the supporting electrolyte and ferrocene as the internal standard (Fig. 5). During the anodic scan in dichloromethane, POAPF and APF underwent oxidation processes, originating from their p-type triphenylamine pendent groups, with onset potentials of 0.46 and 0.42 V, respectively. In contrast, the acceptor-only compound PODPF exhibited no oxidation signal in the positive potential region up to 1.60 V. Upon cathodic sweeping in THF, POAPF and PODPF exhibited reversible reduction waves, arising from their n-type 2,7-bis(diphenylphosphoryl)fluorene segments, with onset potentials of −2.40 and −2.42 eV, respectively. In contrast, the donor-only compound APF exhibited no reduction wave in the cathodic scan up to −3.30 V. Therefore, the sp^3-hybridized carbon atom at the C9 position of the fluorene unit acts as an insulating spacer such that the electrochemical properties of individual p- and n-type groups in POAPF remain essentially unperturbed. Accordingly, the redox behavior of POAPF is similar to a combination of the oxidation behavior of APF and reduction behavior of PODPF. Table 2 lists the corresponding electrochemical data. We also performed a quantum chemical calculation on POAPF at the B3LYP/6-31G* theoretical level (see the Experimental Section for details).[40,41] As depicted in Figure 6, the electron density distributions of the HOMO and LUMO of POAPF are localized predominantly on the electron-rich triphenylamine and electron-deficient 2,7-bis(diphenylphosphoryl)fluorene fragments, respectively, consistent with our original concept of a p/n configuration. Because the oxidation and reduction behavior of POAPF originates from two different functional groups, it is more appropriate to use CV to determine the relative energy levels in such a bipolar molecule rather than the optical method; that is, LUMO = HOMO + $E_{g,abs}$, where $E_{g,abs}$ is the band gap determined merely from the absorption threshold of the triphenylamine component. On the basis of the onset potentials for oxidation and reduction, we estimated the HOMO and LUMO energy levels of POAPF to be −5.26 and −2.40 eV, respectively, with regard to ferrocene (−4.80 eV below vacuum). Consequently, as a host material, POAPF can perform both hole and electron injection functions to achieve more balanced carrier fluxes in the EML relative to those of its donor-only APF and acceptor-only PODPF counterparts. Figure 7 displays the relative

Table 2. Electrochemical properties of the hosts.

host	E_{ox}^{onset} [V]	E_{red}^{onset} [V]	HOMO [eV]	LUMO [eV]	$E_{g,CV}$ [c] [eV]	$E_{g,abs}$ [eV]	E_T [eV]
POAPF	0.46	−2.40	−5.26	−2.40	2.86	3.59	2.75
APF	0.42	N/A	−5.22	−1.62 [b]	N/A	3.60	2.88
PODPF	N/A	−2.42	−6.15 [a]	−2.38	N/A	3.77	2.76

[a] Energy level calculated by subtracting the optical energy gaps from the LUMO energies. [b] Estimated by adding the optical energy gaps to the HOMO energies. [c] Band gap estimated from CV results.

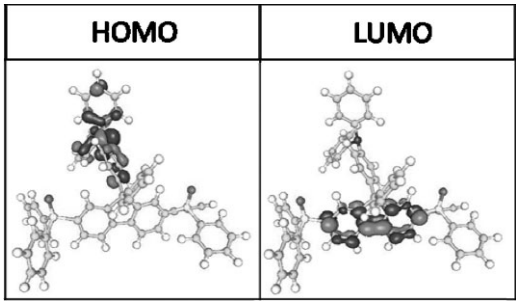

Figure 6. Calculated spatial distributions of the HOMO and LUMO energy densities of POAPF.

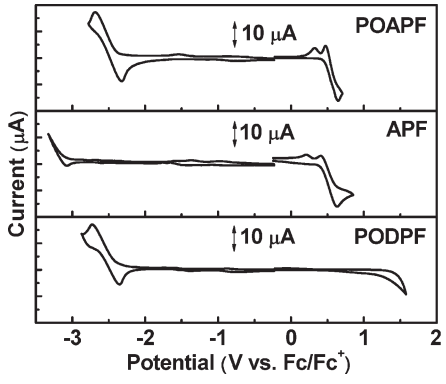

Figure 5. CV results of POAPF, APF, and PODPF.

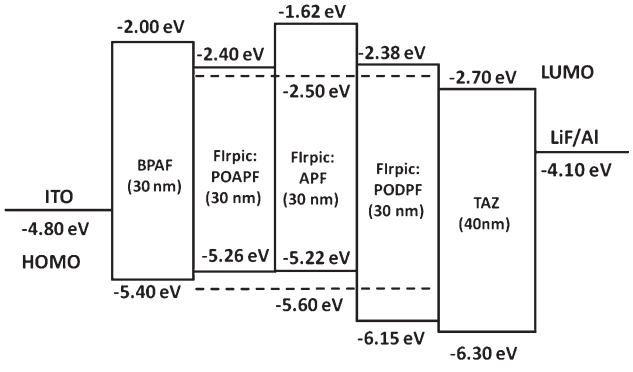

Figure 7. Relative HOMO/LUMO energy levels of the materials used in the devices.

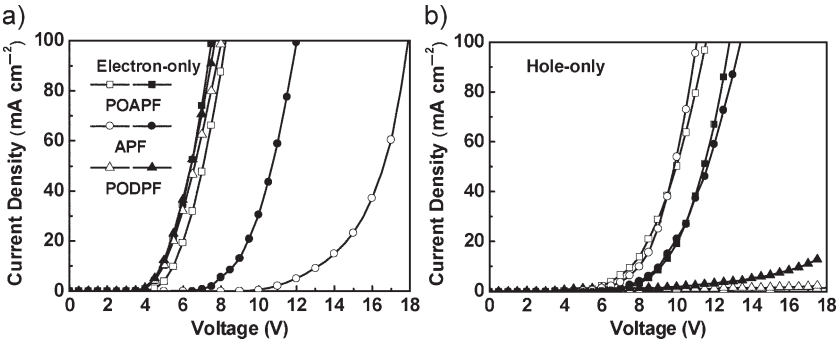

Figure 8. *I–V* characteristics of a) electron- and b) hole-only devices doped with (closed symbols) and without (open symbols) 7 wt% FIrpic.

HOMO/LUMO energy levels of the materials used for the devices; the energy levels of the blue-emitting dopant FIrpic (−5.60/−2.50 eV) were also obtained using the electrochemical method.[43]

2.5. Electroluminescence Properties

To evaluate the suitability of using bipolar POAPF as a host material in blue phosphorescent OLEDs, in initial studies we prepared electron-only devices having the structure indium tin oxide (ITO)/2,9-dimethyl-4,7-diphenyl-1,10-phenanthroline (BCP, 30 nm)/host material (30 nm)/3-(4-biphenylyl)-4-phenyl-5-(4-*tert*-butylphenyl)-1,2,4-triazole (TAZ, 40 nm)/LiF (15 Å)/Al (100 nm) and hole-only devices having the configuration ITO/9,9-bis[4-(*N*,*N*-diphenylamino)phenyl]fluorene (BPAF, 30 nm)/host material (30 nm)/BPAF (40 nm)/Al (100 nm). Here, host material refers to the bipolar POAPF and the two reference unipolar hosts APF and PODPF. For the electron-only devices, the BCP layer, which possesses a large HOMO energy of −6.50 eV, functioned as a hole-blocker to inhibit the majority of holes from being injected from the ITO anode (−4.80 eV) to the organic layer. Thus, the measured current density–voltage (*I–V*) curves refer to the injected electrons. In the case of hole-only devices, because of the large energy injection barrier between the BPAF (LUMO = −2.00 eV) and Al (−4.30 eV) layers, we expected most of the electrons to be impeded. Only holes can be injected from the anode to the organic layers and, therefore, the measured *I–V* characteristics are dominated by holes. Figure 8a and b presents the *I–V* plots of the electron- and hole-only devices, respectively. Generally, p- and n-type materials prefer to accept and transport holes and electrons, respectively. Therefore, the use of unipolar molecules could only effectively mediate either hole or electron injection into the organic layer. Among the *I–V* curves of the undoped electron-only devices (Fig. 8a), we observe that the APF-based device exhibited the highest threshold voltage. Because the large injection barrier (1.08 eV) for electrons between APF (LUMO = −1.62 eV) and TAZ (LUMO = −2.70 eV), electron injection was impeded relative to that in the POAPF- and PODPF-based devices (electron-injection barriers: 0.30 and 0.32 eV, respectively). Likewise, the undoped hole-only device of PODPF exhibited the largest threshold voltage (Fig. 8b). The hole injection was restrained because of the large injection barrier (0.75 eV) for holes from the BPAF (HOMO = −5.40 eV) to PODPF (HOMO = −6.15 eV) layers, relative to that in the POAPF- and APF-based devices (hole-injection barriers: 0.14 and 0.18 eV, respectively). Thus, the incorporation of both donor (triphenylamine) and acceptor (2,7-bis(diphenylphosphoryl)fluorine) units into POAPF provided suitable HOMO and LUMO energy levels for efficient hole- and electron-injection from the charge transporting layers.

Furthermore, we fabricated carrier-only devices doped with 7 wt% FIrpic to investigate the effect of the dopant on the transport characteristics. When POAPF and PODPF were used as hosts, the *I–V* characteristics of the FIrpic-doped, electron-only devices were nearly identical to those of the undoped devices (Fig. 8a), indicating that the presence of FIrpic only minimally affected electron injection. This phenomenon can be explained by considering the energy level diagrams of the devices (Fig. 7), in which the LUMO of the dopant was merely 0.10–0.12 eV lower than that of POAPF or PODPF. Thus, the barriers for electron injected from TAZ to either FIrpic or the hosts were almost identical. On the other hand, when APF was used as the host material, the required voltage of the doped device at a given current density was lower than that of the undoped counterpart, revealing the facilitation of electron injection by the doped low-LUMO-lying FIrpic. In the case of the hole-only devices (Fig. 8b), we noted that the HOMO energy level of FIrpic was deeper than those of the hosts APF and POAPF. Consequently, hole injection in the doped devices was impeded and the drift velocity of holes was lowered, presumably because of the scattering of dopant sites,[44] resulting in higher threshold voltages relative to those of their undoped reference devices. In contrast, the *I–V* curve of the doped PODPF device was steeper than that of the undoped counterpart, because the doping of the relatively shallower HOMO-lying FIrpic would lower the energy barrier for hole injection.[45] Figure 8 reveals that although the doping of FIrpic changed the *I–V* characteristics of the carrier-only devices, the bipolar host POAPF (the major component of the EML) remained the predominant factor facilitating both hole and electron injection.

Next, we doped the bipolar host material POAPF with a commercially available triplet blue emitter, FIrpic, to realize devices exhibiting highly efficient blue electrophosphorescence. The device structure had the configuration ITO/BPAF (30 nm)/EML (30 nm)/TAZ (40 nm)/LiF (15 Å)/Al (100 nm). Here, EML refers to the layer of POAPF doped with 7 wt% FIrpic; BPAF[46] and TAZ were employed as hole- and electron-transporting layers, respectively. The values of E_T of BPAF (2.87 eV, estimated from the phosphorescent spectra measured in 2-methyltetrahydrofuran at 77 K) and TAZ (2.70 eV)[47] were sufficiently high to prevent any possible luminescence quenching by the carrier-transporting layers and to confine the triplet excitons in the EML.[48,49] For comparison, we also fabricated the corresponding devices incorporating APF, PODPF, and the conventional material *N*,*N*′-dicarbazolyl-3,5-benzene (mCP), respectively, as hosts. Figure 9 displays the current density–voltage–luminance (*I–V–L*) characteristics of these blue-light-emitting devices. The POAPF-based device exhibited a significantly lower operating voltage than those of the reference devices at the same current density. We attribute the enhanced device current to the facilitation of both hole and

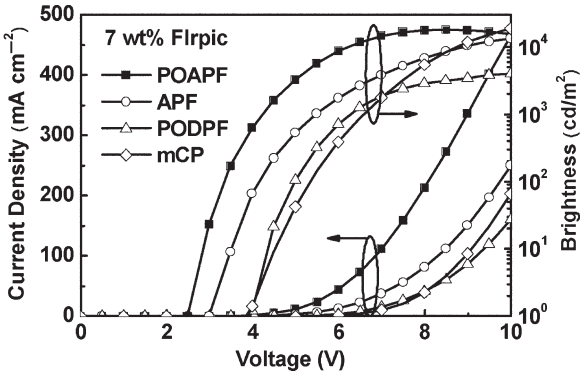

Figure 9. *I–V–L* characteristics of FIrpic-doped devices.

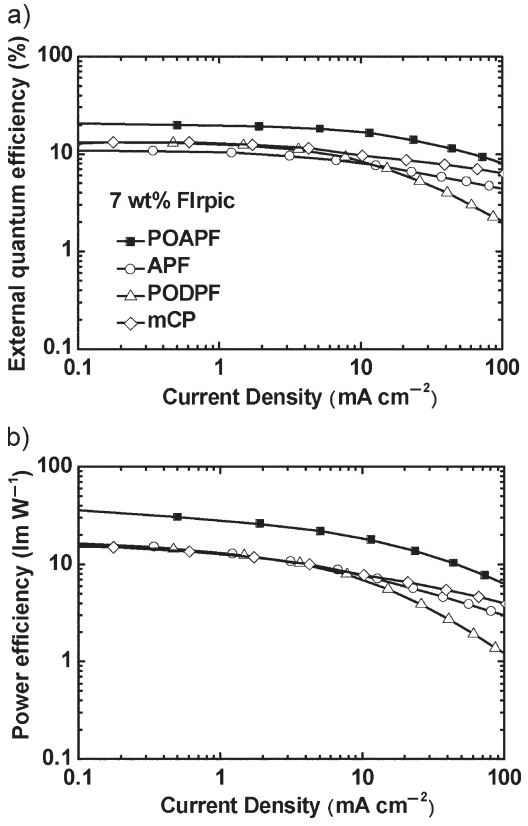

Figure 10. Plots of a) EQE and b) PE with respect to current density for the FIrpic-doped devices.

electron injection when using bipolar POAPF as the host material, as revealed for the carrier-only devices (vide supra). The diode based on POAPF exhibited a relatively low turn-on voltage of 2.5 V (corresponding to 1 cd m^{-2}). At the practical brightnesses of 100 and 1000 cd m^{-2}, the driving voltages of the POAPF-based device were merely 3.3 and 4.2 V, respectively. Figure 10 displays the external quantum efficiency (EQE) and power efficiency (PE) plotted with respect to the current density. The POAPF-based device achieved an EQE as high as 20.6% (0.07 mA cm^{-2} and 24 cd m^{-2}), almost a twofold enhancement over those of the reference counterparts (10.8% for APF, 13.2% for PODPF, and 13.2% for mCP). This value of 20.6% is almost equal to the theoretical limit of 20% for phosphorescent OLEDs, suggesting that the use of a bipolar host material results in balanced charge fluxes within the EML to achieve a higher EQE than that in devices incorporating unipolar host molecules. The combination of such a low driving voltage and a high EQE of the POAPF-based device also resulted in a high PE of 36.7 lm W^{-1}. It is notable that these efficiencies remained high at 20.2% (33.8 lm W^{-1}) and 18.8% (24.3 lm W^{-1}) at brightnesses of 100 and 1000 cd m^{-2}, respectively. These values are much higher than that of the device based on the conventionally used material mCP and are among the highest ever reported for FIrpic-doped devices.[28,33,47–50] Table 3 lists the key characteristics of the blue electrophosphorescence obtained using the various host materials. In addition to the efficient carrier-injection in the POAPF-based device, we also attribute the high efficiencies to the effective carrier/exciton confinement within the EML. The electroluminescence (EL) emission spectra of the POAPF-based device over the entire range of operating voltages (Fig. 11) reveal the same blue emission with a maximum intensity at 474 nm, and Commission Internationale de L'Eclairage (CIE) coordinates of (0.13, 0.27), assigned to the triplet emission of FIrpic.[13,22] We observed no emission originating from adjacent organic layers, indicating that BPAF and TAZ functioned as effective blockers to confine carriers and excitons within the EML.

Table 3. EL data for the FIrpic-doped devices.

host	POAPF	APF	PODPF	mCP
V [a] [V]	2.5; 3.3; 4.2	3.0; 4.1; 5.5	3.9; 5.0; 6.3	3.8; 5.3; 6.6
EQE [%][b]	20.6; 20.2; 18.8	10.8; 10.6; 8.7	13.2; 12.9; 10.1	13.2; 13.1; 11.2
PE [lm W^{-1}][b]	36.7; 33.8; 24.3	16.9; 14.6; 8.9	16.1; 14.3; 9.0	14.9; 14.1; 9.6
LE [cd A^{-1}][b]	35.4; 34.8; 32.3	19.2; 18.9; 15.4	23.0; 22.6; 17.8	23.7; 23.6; 20.1
CIE [*x*, *y*][c]	0.13, 0.27	0.13, 0.28	0.13, 0.28	0.12, 0.29

[a] Order of operating voltages: 1, 100, 1000 cd m^{-2}. [b] Order of measured values: maximum value, then values at 100 and 1000 cd m^{-2}. [c] Measured at 7 V.

Recently, it has been demonstrated that an interfacial interaction between the Al metal and the phosphonate groups can facilitate efficient electron injection from the Al cathode to the phosphonate-containing material.[51] Thus, we were interested in fabricating a simple double-layer EL device having the architecture

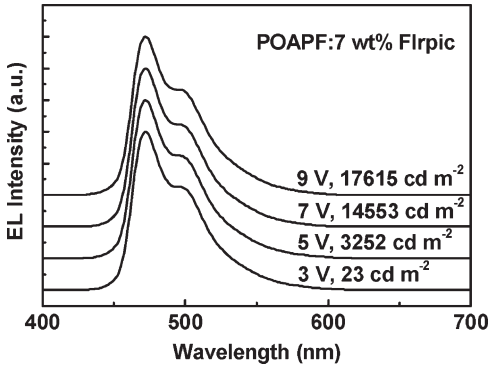

Figure 11. EL spectra of the POAPF-based device under various operating voltages.

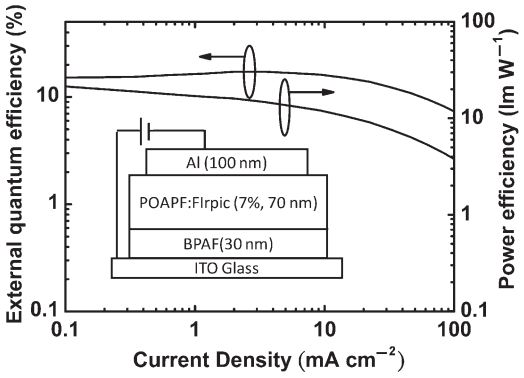

Figure 12. Variations in the EQE and PE plotted with respect to the current density for the POAPF double-layer device. Inset: device structure.

ITO/BPAF (30 nm)/POAPF:7 wt% FIrpic (70 nm)/Al (100 nm), where POAPF was used simultaneously as the host and as an electron-transporting and injecting material. Figure 12 presents plots of the EQE and PE with respect to the current density of the POAPF-based double-layer device. This simple device exhibited peak EL efficiencies of 17.2% and 21.2 lm W^{-1}. Even at a practical brightness of 1000 cd m^{-2}, the efficiencies of this double-layer device remained as high as 17.1% and 14.9 lm W^{-1}. The application of simple devices providing high efficiency is expected to reduce the overall cost and increase the extent of OLED commercialization. We ascribe the reduced EL efficiencies, relative to those of the multilayer device, to less efficient charge recombination and/or reduced hole/exciton confinement as a result of the absence of the TAZ and LiF layers. Nevertheless, the resulting EL efficiencies of this simple double-layer device still rival those of the multilayer devices based on APF, PODPF, and conventional host materials.[12,13,22–27]

3. Conclusions

We have developed a novel bipolar host, POAPF, comprising an electron-donor triphenylamine unit and an electron-acceptor diphenylphosphoryl-substituted fluorene unit. Because the triphenylamine and 2,7-bis(diphenylphosphoryl)fluorene segments were connected through the sp^3-hybridized C9 atom of the fluorene unit, thereby eliminating extended π-conjugation, POAPF possessed a high triplet energy of 2.75 eV. Electrochemistry studies with related carrier-only devices revealed that the bipolar character of POAPF did indeed improve the charge injection for both hole and electron carriers relative to those of its unipolar counterparts to achieve balanced charge fluxes. These features allowed us to fabricate highly efficient blue electrophosphorescent devices using POAPF as the host material. The 7 wt% FIrpic-doped device exhibited a very low turn-on voltage (2.5 V) along with EL efficiencies reaching as high as 20.6% and 36.7 lm W^{-1}. Even in simple double-layer devices incorporating POAPF simultaneously as the host and electron-transporting and -injecting material, the EL efficiencies remained satisfactory (17.2% and 21.2 lm W^{-1}). These results indicate that the design of bipolar host materials featuring isolated donor and acceptor functionalities is an effective strategy toward improving the performance of OLEDs for use in next-generation flat-panel displays and light sources.

4. Experimental

Materials: **1** [36], 9-phenyl-9-fluorenol [52], and 2,7-dibromo-9,9-diphenylfluorene [53] were prepared by reported procedures. The solvents were dried using standard procedures. All other reagents were used as received from commercial sources unless otherwise stated.

Characterization: ^{1}H, ^{13}C, and ^{31}P NMR spectra were recorded using Varian UNITY INOVA 500 MHz and Varian UNITY 300 MHz spectrometers. Mass spectra and high-resolution mass spectra (HRMS) were obtained using JEOL JMS-HX 110 and Finnigan Thermo Quest MAT 95XL mass spectrometers. DSC was performed using a SEIKO EXSTAR 6000DSC unit operated at heating and cooling rates of 10 and 50 °C min^{-1}, respectively. The glass transition temperatures (T_g) were determined from the second heating scan. TGA was undertaken using a DuPont TGA 2950 instrument. The thermal stabilities of the samples under nitrogen atmosphere were determined by measuring their weight losses while heating at a rate of 20 °C min^{-1}. UV–Vis spectra were measured using an HP 8453 diode-array spectrophotometer. PL spectra were obtained using a Hitachi F4500 luminescence spectrometer. The quantum yields of the hosts in various solvents were determined using quinine sulfate (quantum yield: 0.53 ± 0.02 (in 0.1 N H_2SO_4)) [54] as the fluorescence standard. Sample concentrations for quantum yield measurements were set at 5×10^{-6} M to eliminate self-absorption and quenching effects. The low-temperature phosphorescence spectra were obtained using a composite spectrometer containing a monochromator (Jobin Yvon, Triax 190) coupled with a liquid nitrogen-cooled charge-coupled device (CCD) detector (Jobin Yvon, CCD-1024x256-open-1LS). Nanosecond lifetime measurements were recorded using a photon-counting system with a hydrogen-filled lamp as the excitation source. The emission decays were analyzed through the sum of exponential functions, which allows partial removal of the instrument time broadening and, consequently, renders a temporal resolution of ca. 200 ps. The picosecond dynamical lifetime studies were performed using a Ti-Sapphire oscillator operated at 700–1050 nm (82 MHz, Spectra Physics) as the excitation source. The fundamental train of pulses was typically pulse-selected (Neos, model N17389) to 0.8–8 MHz to reduce the repetition rate, and then used to produce second harmonics as an excitation light source. A polarizer was placed in the emission path to ensure that the polarization of the fluorescence was set at the magic angle (54.7°) with respect to that of the pump laser to eliminate fluorescence anisotropy. An Edinburgh OB 900-L time-correlated single-photon counting system was used as a detecting system, providing a temporal resolution of ca. 15 ps. CV measurements were performed using a BAS 100 B/W electrochemical analyzer operated at a scan rate of 100 mV s^{-1}. The potentials were measured against a Ag/Ag$^+$ (0.01 M $AgNO_3$) reference electrode using ferrocene/ferrocenium (Fc/Fc^+) as an internal standard.

Computational Methodology: The structure of POAPF was calculated at the B3LYP/6-31G* level of theory [40]. After obtaining the converged geometry, a vibrational frequency analysis was performed to confirm that the imaginary frequency number was zero, which was expected to be a minimum. To obtain the radius of the solvent cavity, the keyword volume was used; the recommend value was adopted directly in this study. All calculations were performed using the Gaussian 03 program [41].

Fabrication of OLEDs: The EL devices were fabricated through vacuum deposition of the materials at 10^{-6} torr onto ITO glass having a sheet resistance of 25 Ω square^{-1}. All of the organic layers were deposited at a rate of 1.0 Å s^{-1}. The cathode was completed through thermal deposition of LiF at a deposition rate of 0.1 Å s^{-1}, then capped with Al metal through thermal evaporation at a rate of 4.0 Å s^{-1}. The relationships of the current density and brightness of the devices with respect to voltage were

measured using a Keithley 2400 source meter and a Newport 1835C optical meter equipped with an 818ST silicon photodiode. The EL spectrum was obtained using a Hitachi F4500 luminescence spectrometer.

2: CF_3SO_3H (0.90 mL, 10.2 mmol) was added dropwise to a solution of triphenylamine (3.35 g, 13.7 mmol) and 2,7-dibromo-9-phenyl-9-fluorenol (2.85 g, 6.85 mmol) in dichloromethane (100 mL). The reaction mixture was stirred for 30 min at room temperature before being quenched with saturated aqueous $NaHCO_3$ (100 mL). The organic phase was washed twice with water (100 mL) and then dried ($MgSO_4$). After evaporation of the volatiles, the residue was purified through column chromatography (SiO_2; EtOAc/hexane 1:10) to yield **2** as a white solid (3.61 g, 82%). ^{1}H NMR (300 MHz, [d_8]THF, δ): 7.75 (d, J = 8.1 Hz, 2H), 7.60 (d, J = 1.5 Hz, 1H), 7.53 (dd, J = 8.1, 1.8 Hz, 2H), 7.25–7.15 (m, 9H), 7.07–7.03 (m, 6H), 7.00–6.95 (m, 2H), 6.91 (d, J = 8.7 Hz, 2H); ^{13}C NMR (75 MHz, [d_8]THF, δ): 155.03, 149.17, 148.42, 146.35, 139.78, 139.24, 132.37, 130.75, 130.64, 130.26, 129.85, 129.33, 128.39, 126.08, 124.47, 124.09, 123.40, 123.10, 66.79; EIMS (m/z): 643 [M^+].

POAPF: *n*-Butyllithium (4.00 mL, 10.0 mmol, 2.5 M in hexane) was added dropwise to a stirred solution of **2** (2.75 g, 4.28 mmol) in anhydrous THF (200 mL) at −78 °C under a nitrogen atmosphere. After stirring at −78 °C for a further 3 h, chlorodiphenylphosphine (2.00 mL, 10.9 mmol) was added to give a clear, pale-yellow solution. The mixture was gradually warmed to room temperature over 4 h while stirring. The reaction mixture was quenched with water (200 mL) and then extracted with EtOAc (2 × 100 mL). The combined extracts were dried ($MgSO_4$) and then concentrated under reduced pressure. The crude product was dissolved in dichloromethane (150 mL) and then 30% aqueous hydrogen peroxide (30 mL) was added. The mixture was stirred at room temperature for 3 h and then extracted with dichloromethane (3 × 50 mL). The collected organic phases were dried ($MgSO_4$) and then concentrated under reduced pressure. The residue was purified through column chromatography (SiO_2; EtOAc/MeOH 50:1) to yield POAPF as a white solid (2.69 g, 71%). ^{1}H NMR (300 MHz, [d_8]THF, δ): 8.02 (dd, J = 7.8, 2.4 Hz, 2H), 7.81 (d, J = 11.7 Hz, 2H), 7.75 (dd, J = 11.4, 7.8 Hz, 2H), 7.67–7.59 (m, 8H), 7.50–7.44 (m, 4H), 7.41–7.35 (m, 8H), 7.24–7.19 (m, 4H), 7.15–7.09 (m, 5H), 7.02–6.98 (m, 6H), 6.96–6.92 (m, 2H), 6.83 (d, J = 8.7 Hz, 2H); ^{13}C NMR (75 MHz, [d_8]THF, δ): 153.30 (d, J (C,P) = 12.0 Hz), 149.21, 148.24, 146.35, 143.84, 139.88, 135.73 (d, J (C,P) = 101.1 Hz), 135.64 (d, J (C,P) = 102.2 Hz), 133.34 (d, J (C,P) = 9.5 Hz), 133.19 (d, J (C,P) = 13.6 Hz), 132.84, 131.51 (d, J (C,P) = 10.5 Hz), 130.63, 130.04, 129.74, 129.66 (d, J (C,P) = 11.6 Hz), 129.18, 128.29, 125.77, 124.55, 124.33, 122.42 (d, J (C,P) = 13.1 Hz), 66.69; ^{31}P NMR (202 MHz, [d_8]THF, δ): 25.98. HRMS (FAB, m/z): [M + H]$^+$ calcd for $C_{61}H_{46}NO_2P_2$, 886.3004; found, 886.3011. Anal. calcd for $C_{61}H_{45}NO_2P_2$: C 82.70, H 5.12, N, 1.58; found: C 82.67, H 5.17, N 1.56.

APF: Prepared as a white solid (2.89 g, 75%) in the same manner as **2**, from triphenylamine (3.93 g, 16.0 mmol) and 9-phenyl-9-fluorenol (2.05 g, 7.94 mmol). ^{1}H NMR (300 MHz, [d_8]THF, δ): 7.80 (d, J = 7.5 Hz, 2H), 7.43 (d, J = 7.2 Hz, 2H), 7.32 (dt, J = 7.5, 1.2 Hz, 2H), 7.24 (dd, J = 7.2, 1.2 Hz, 2H), 7.21–7.12 (m, 9H), 7.08 (d, J = 8.7 Hz, 2H), 7.03–6.99 (m, 4H), 6.97–6.91 (m, 2H), 6.88 (d, J = 8.7 Hz, 2H); ^{13}C NMR (75 MHz, [d_8]THF, δ): 152.93, 149.33, 147.88, 147.79, 141.73, 141.32, 130.55, 130.41, 129.46, 129.44, 128.93, 128.76, 127.81, 127.62, 125.71, 124.43, 124.16, 121.47, 66.53; HRMS (EI, m/z): [M^+] calcd for $C_{37}H_{27}N$, 485.2144; found, 485.2137. Anal. calcd for $C_{37}H_{27}N$: C 91.51, H 5.60, N 2.88; found: C 91.36, H 5.58, N 2.87.

PODPF: Prepared as a white solid (2.61 g, 78%) in the same manner as POAPF, from 2,7-dibromo-9,9-diphenylfluorene (2.23 g, 4.67 mmol). ^{1}H NMR (300 MHz, [d_8]THF, δ): 8.02 (dd, J = 7.8, 2.1 Hz, 2H), 7.79 (d, J = 12.0 Hz, 2H), 7.74–7.68 (m, 2H), 7.62 (dd, J = 11.4, 8.1 Hz, 8H), 7.48 (t, J = 7.2 Hz, 4H), 7.41–7.36 (m, 8H), 7.17–7.03 (m, 10H); ^{13}C NMR (75 MHz, [d_8]THF, δ): 153.07 (d, J (C,P) = 12.5 Hz), 146.33, 143.93, 135.76 (d, J (C,P) = 101.2 Hz), 135.62 (d, J (C,P) = 102.2 Hz), 133.34 (d, J (C,P) = 9.5 Hz), 133.20 (d, J (C,P) = 11.0 Hz), 132.83, 131.57 (d, J (C,P) = 10.1 Hz), 129.73, 129.65 (d, J (C,P) = 12.0 Hz), 129.21, 128.29, 122.41 (d, J (C,P) = 12.5 Hz), 67.16; ^{31}P NMR (202 MHz, [d_8]THF, δ): 25.52; HRMS (FAB, m/z): [M + H]$^+$ calcd for $C_{49}H_{37}O_2P_2$, 719.2269; found, 719.2268. Anal. calcd for $C_{49}H_{36}O_2P_2$: C 81.88, H 5.05; found: C 81.58, H 5.03.

Acknowledgements

We thank the National Science Council for financial support. Our special thanks go to Professor C.-H. Cheng for his support and assistance during the preparation and characterization of the light-emitting devices. Supporting information is available online at Wiley InterScience or from the author.

Received: April 22, 2009
Published online: July 24, 2009

[1] C. W. Tang, S. A. VanSlyke, *Appl. Phys. Lett.* **1987**, *51*, 913.
[2] M. A. Baldo, D. F. O'Brien, Y. You, A. Shoustikov, S. Sibley, M. E. Thompson, S. R. Forrest, *Nature* **1998**, *395*, 151.
[3] A. Köhler, J. S. Wilson, R. H. Friend, *Adv. Mater.* **2002**, *14*, 701.
[4] W. S. Huang, J. T. Lin, C. H. Chien, Y. T. Tao, S. S. Sun, Y. S. Wen, *Chem. Mater.* **2004**, *16*, 2480.
[5] J. Ding, J. Gao, Y. Cheng, Z. Xie, L. Wang, D. Ma, X. Jing, F. Wang, *Adv. Funct. Mater.* **2006**, *16*, 575.
[6] T. Tsuzuki, S. Tokito, *Adv. Mater.* **2007**, *19*, 276.
[7] E. Orselli, R. Q. Albuquerque, P. M. Fransen, R. Fröhlich, H. M. Janssen, L. D. Cola, *J. Mater. Chem.* **2008**, *18*, 4579.
[8] M. A. Baldo, C. Adachi, S. R. Forrest, *Phys. Rev. B* **2000**, *62*, 10967.
[9] M. A. Baldo, M. E. Thompson, S. R. Forrest, *Nature* **2000**, *403*, 750.
[10] V. I. Adamovich, S. R. Cordero, P. I. Djurovich, A. Tamayo, M. E. Thompson, B. W. D'Andrade, S. R. Forrest, *Org. Electron.* **2003**, *4*, 77.
[11] M. Sudhakar, P. I. Djurovich, T. E. Hogen-Esch, M. E. Thompson, *J. Am. Chem. Soc.* **2003**, *125*, 7796.
[12] R. J. Holmes, S. R. Forrest, Y. J. Tung, R. C. Kwong, J. J. Brown, S. Garon, M. E. Thompson, *Appl. Phys. Lett.* **2003**, *82*, 2422.
[13] S. Tokito, T. Iijima, Y. Suzuri, H. Kita, T. Tsuzuki, F. Sato, *Appl. Phys. Lett.* **2003**, *83*, 569.
[14] H. Inomata, K. Goushi, T. Masuko, T. Konno, T. Imai, H. Sasabe, J. J. Brown, C. Adachi, *Chem. Mater.* **2004**, *16*, 1285.
[15] M. Guan, Z. Chen, Z. Bian, Z. Liu, Z. Gong, W. Baik, H. Lee, C. Huang, *Org. Electron.* **2006**, *7*, 330.
[16] G. Hughes, M. R. Bryce, *J. Mater. Chem.* **2005**, *15*, 94.
[17] C. T. Chen, Y. Wei, J. S. Lin, M. V. R. K. Moturu, W. S. Chao, Y. T. Tao, C. H. Chien, *J. Am. Chem. Soc.* **2006**, *128*, 10992.
[18] N. J. Lundin, A. G. Blackman, K. C. Gordon, D. L. Officer, *Angew. Chem. Int. Ed.* **2006**, *45*, 2582.
[19] S. Tokito, H. Tanaka, A. Okada, Y. Taga, *Appl. Phys. Lett.* **1996**, *69*, 878.
[20] S. Tokito, K. Noda, H. Fujikawa, Y. Taga, M. Kimura, K. Shimada, Y. Sawaki, *Appl. Phys. Lett.* **2000**, *77*, 160.
[21] M. A. Baldo, S. Lamansky, P. E. Burrows, M. E. Thompson, S. R. Forrest, *Appl. Phys. Lett.* **1999**, *75*, 4.
[22] S. J. Yeh, M. F. Wu, C. T. Chen, Y. H. Song, Y. Chi, M. H. Ho, S. F. Hsu, C. H. Chen, *Adv. Mater.* **2005**, *17*, 285.
[23] M. H. Tsai, H. W. Lin, H. C. Su, T. H. Ke, C. C. Wu, F. C. Fang, Y. L. Liao, K. T. Wong, C. I. Wu, *Adv. Mater.* **2006**, *18*, 1216.
[24] M. H. Tsai, Y. H. Hong, C. H. Chang, H. C. Su, C. C. Wu, A. Matoliukstyte, J. Simokaitiene, S. Grigalevicius, J. V. Grazulevicius, C. P. Hsu, *Adv. Mater.* **2007**, *19*, 862.
[25] D. R. Whang, Y. You, S. H. Kim, W. I. Jeong, Y. S. Park, J. J. Kim, S. Y. Park, *Appl. Phys. Lett.* **2007**, *91*, 233501.
[26] P. E. Burrows, A. B. Padmaperuma, L. S. Sapochak, P. Djurovich, M. E. Thompson, *Appl. Phys. Lett.* **2006**, *88*, 183503.
[27] A. B. Padmaperuma, L. S. Sapochak, P. E. Burrows, *Chem. Mater.* **2006**, *18*, 2389.
[28] X. Cai, A. B. Padmaperuma, L. S. Sapochak, P. A. Vecchi, P. E. Burrows, *Appl. Phys. Lett.* **2008**, *92*, 083308.
[29] Y. Tao, Q. Wang, C. Yang, Q. Wang, Z. Zhang, T. Zou, J. Qin, D. Ma, *Angew. Chem. Int. Ed.* **2008**, *47*, 8104.
[30] Z. Ge, T. Hayakawa, S. Ando, M. Ueda, T. Akiike, H. Miyamoto, T. Kajita, M.-A. Kakimoto, *Adv. Funct. Mater.* **2008**, *18*, 584.

[31] Z. Ge, T. Hayakawa, S. Ando, M. Ueda, T. Akiike, H. Miyamoto, T. Kajita, M.-A. Kakimoto, *Org. Lett.* **2008**, *10*, 421.
[32] M. Y. Lai, C. H. Chen, W. S. Huang, J. T. Lin, T. H. Ke, L. Y. Chen, M. H. Tsai, C. C. Wu, *Angew. Chem. Int. Ed.* **2008**, *47*, 581.
[33] S. J. Su, H. Sasabe, T. Takeda, J. Kido, *Chem. Mater.* **2008**, *20*, 1691.
[34] P. J. Low, M. A. J. Paterson, D. S. Yufit, J. A. K. Howard, J. C. Cherryman, D. R. Tackley, R. Brook, B. Brown, *J. Mater. Chem.* **2005**, *15*, 2304.
[35] R. D. Burkhart, N. I. Jhon, *J. Phys. Chem.* **1991**, *95*, 7189.
[36] C. H. Chien, P. I. Shih, F. I. Wu, C. F. Shu, Y. Chi, *J. Polym. Sci. Part A: Polym. Chem.* **2007**, *45*, 2073.
[37] K. A. Watson, F. L. Palmieri, J. W. Connell, *Macromolecules* **2002**, *35*, 4968.
[38] Y. Y. Chien, K. T. Wong, P. T. Chou, Y. M. Cheng, *Chem. Commun.* **2002**, 2874.
[39] K. T. Wong, S. Y. Ku, Y. M. Cheng, X. Y. Lin, Y. Y. Hung, S. C. Pu, P. T. Chou, G. H. Lee, S. M. Peng, *J. Org. Chem.* **2006**, *71*, 456.
[40] A. D. Becke, *J. Chem. Phys.* **1993**, *98*, 5648.
[41] M. J. Frisch, G. W. Trucks, H. B. Schlegel, G. E. Scuseria, M. A. Robb, J. R. Cheeseman, J. A. Montgomery, Jr, T. Vreven, K. N. Kudin, J. C. Burant, J. M. Millam, S. S. Iyengar, J. Tomasi, V. Barone, B. Mennucci, M. Cossi, G. Scalmani, N. Rega, G. A. Petersson, H. Nakatsuji, M. Hada, M. Ehara, K. Toyota, R. Fukuda, J. Hasegawa, M. Ishida, T. Nakajima, Y. Honda, O. Kitao, H. Nakai, M. Klene, X. Li, J. E. Knox, H. P. Hratchian, J. B. Cross, C. Adamo, J. Jaramillo, R. Gomperts, R. E. Stratmann, O. Yazyev, A. J. Austin, R. Cammi, C. Pomelli, J. W. Ochterski, P. Y. Ayala, K. Morokuma, G. A. Voth, P. Salvador, J. J. Dannenberg, V. G. Zakrzewski, S. Dapprich, A. D. Daniels, M. C. Strain, O. Farkas, D. K. Malick, A. D. Rabuck, K. Raghavachari, J. B. Foresman, J. V. Ortiz, Q. Cui, A. G. Baboul, S. Clifford, J. Cioslowski, B. B. Stefanov, G. Liu, A. Liashenko, P. Piskorz, I. Komaromi, R. L. Martin, D. J. Fox, T. Keith, M. A. Al-Laham, C. Y. Peng, A. Nanayakkara, M. Challacombe, P. M. W. Gill, B. Johnson, W. Chen, M. W. Wong, C. Gonzalez, J. A. Pople, *Gaussian 03*, Gaussian, Inc, Wallingford, CT **2004**.
[42] T. J. Kanh, M. A. Kahkow, M. D. Giser, S. Swallen, V. Nagarajan, W. Jarzeba, P. F. Barbara, *J. Phys. Chem.* **1998**, *92*, 6800.
[43] J. J. Brooks, R. C. Kwong, Y. J. Tung, M. S. Weaver, B. D'Andrade, V. Adamovich, M. E. Thompson, S. R. Forrest, J. J. Brown, *Proc. SPIE* **2004**, *5519*, 35.
[44] Y. S. Park, J. W. Kang, D. M. Kang, J. W. Park, Y. H. Kim, S. K. Kwon, J. J. Kim, *Adv. Mater.* **2008**, *20*, 1957.
[45] M. T. Lee, J. S. Lin, M. T. Chu, M. R. Tseng, *Appl. Phys. Lett.* **2008**, *92*, 173305.
[46] M. E. El-Khouly, *Spectrochim. Acta, Part A* **2007**, *67*, 636.
[47] L. Xiao, S. J. Su, Y. Agata, H. Lan, J. Kido, *Adv. Mater.* **2009**, *21*, 1271.
[48] N. Chopra, J. Lee, Y. Zheng, S. H. Eom, J. Xue, F. So, *Appl. Phys. Lett.* **2008**, *93*, 143307.
[49] J. Lee, N. Chopra, S. H. Eom, Y. Zheng, J. Xue, F. So, J. Shi, *Appl. Phys. Lett.* **2008**, *93*, 123306.
[50] D. Tanaka, Y. Agata, T. Takeda, S. Watanabe, J. Kido, *Jpn. J. Appl. Phys.* **2007**, *46*, L117.
[51] G. Zhou, Y. Geng, Y. Cheng, Z. Xie, L. Wang, X. Jing, F. Wang, *Appl. Phys. Lett.* **2006**, *89*, 233501.
[52] P. I. Shih, C. L. Chiang, A. K. Dixit, C. K. Chen, M. C. Yuan, R. Y. Lee, C. T. Chen, E. W. G. Diau, C. F. Shu, *Org. Lett.* **2006**, *8*, 2799.
[53] Z. Q. Gao, Z. H. Li, P. F. Xia, M. S. Wong, K. W. Cheah, C. H. Chen, *Adv. Funct. Mater.* **2007**, *17*, 3194.
[54] M. J. Adams, J. G. Highfield, G. F. Kirkbright, *Anal. Chem.* **1977**, *49*, 1850.